# A New Wide-area Monitoring System of Electromagnetic Fields around Megawatt-class Amplifiers for Ion Cyclotron Range of Frequency Heating at a Fusion Test Facility

# A New Wide-area Monitoring System of Electromagnetic Fields around Megawatt-class Amplifiers for Ion Cyclotron Range of Frequency Heating at a Fusion Test Facility

Masahiro Tanaka, Tetsuo Seki, Jianqing Wang, *fellow, IEEE*,
Yoshitsugu Kamimura, *Member, IEEE,* Tatsuhiko Uda, and Osamu Fujiwara, *Life Member, IEEE*

***Abstract*—Nuclear fusion research requires the production of high-temperature plasma. One of the plasma heating methods is the use of radiofrequency (RF) waves. The RF wave heating system uses a high-power amplifier, which poses a concern about the leakage electromagnetic fields. Therefore, a new wide-area multipoint electromagnetic monitoring system using personal RF monitors has been developed. The developed monitoring system was applied to the megawatt-class amplifiers for the "Ion Cyclotron Range of Frequency" (ICRF) heating system in the frequency range of ion cyclotron resonance from 30 to 40 MHz. As a result, the leakage magnetic field was less than the measurement sensitivity during the plasma experiment, in which the leakage electric field was detected with sufficient sensitivity. The leakage electric field becomes larger as the RF forward power increases, and thus the electric field would be radiated through the stub and/or high voltage supply line connected to the anode of tetrode in the ICRF amplifier. The electric field around the ICRF amplifiers did not exceed the reference level of ICNIRP. The developed wide-area multipoint monitoring system will be useful for monitoring the leakage RF electromagnetic fields around the ICRF heating system at the future fusion devices.**

***Index Terms*—Electromagnetic fields, fusion test device, ion cyclotron range of frequency heating system, high-power amplifier, non-ionization radiation monitoring, safety management,**

## I. Introduction

The nuclear fusion reactor as one of the new energy sources will be directly associated with the life of human beings in the near future. To realize a nuclear fusion reactor on the earth, high temperature (10~30 keV) plasma is required to become close enough for the nuclear fusion reactions to occur. Also, the confinement of plasma long enough with sufficient pressure is necessary. These two conditions must be fulfilled simultaneously. For the understanding of plasma physics, high-performance plasma, which has a high temperature and high density and high confinement time of plasma, must be generated in a vacuum vessel with a high magnetic field. To produce high-temperature plasma, a magnetic confinement fusion test device has some auxiliary heating systems, i.e., Neutral Beam Injection (NBI), Electron Cyclotron Resonance Heating (ECRH) and Ion Cyclotron Range of Frequency (ICRF) heating. Among these heating systems, ECRH and ICRF heating use electromagnetic waves in the order of a few ten MHz to a few hundred GHz. In the presence of a uniform magnetic field, a charged particle is known to undergo cyclotron gyration with a characteristic cyclotron frequency. Dynamic effects such as cyclotron gyration lead to the possibility of wave resonance in the plasma [1, 2]. Therefore, the electron and ion resonance heating systems are used in magnetic confinement fusion test devices.

To progress the nuclear fusion research, various fusion test devices have been constructed and operated all over the world. Some of the large fusion test devices such as Tokamak Fusion Test Reactor and Joint European Torus have successfully produced fusion powers of more than 10 MW by deuterium-tritium reaction using the injection of large heating power [3, 4]. In these large fusion test facilities, the total power of the plasma heating system becomes a few ten megawatts. During the plasma experiment, ionization radiation such as neutrons, X-ray is emitted. Therefore, the plasma experimental hall is a radiation controlled area and access is restricted. On the other hand, the power supply for the plasma heating equipment is located in a non-radiation controlled area, which allows

This work is performed with the support and under the auspices of the NIFS Collaboration Research Program (NIFS20KLEA045), and partially supported by JSPS KAKENHI Grand No. JP20360132.

Masahiro Tanaka is with the National Institute for Fusion Science and the Graduate University for Advanced Studies, SOKENDAI, Toki, Gifu, Japan (e-mail: tanaka.masahiro@nifs.ac.jp).

Testuo Seki is with the National Institute for Fusion Science, Toki, Gifu, Japan (e-mail: seki.tetsuo@nifs.ac.jp).

Jianqing Wang is with the Department of Electrical and Mechanical Engineering, Nagoya Institute of Technology, Nagoya, Aichi, Japan (e-mail: wang@nitech.ac.jp).

Yoshitsugu Kamimura is with the Department of Information Science, Utsunomiya University, Utsunomiya, Tochigi, Japan (e-mail: gami@is.utsunomiya-u.ac.jp).

Tatsuhiko Uda is the professor emeritus of the National Institute for Fusion Science and the Graduate University for Advanced Studies, SOKENDAI, (e-mail: uda.tatsuhiko@toki-fs.jp).

Osamu Fujiwara is the professor emeritus of the Nagoya Institute of Technology (e-mail: fujiwara.osamu@nitech.ac.jp).

workers' to enter. Non-ionizing radiation such as the leakage of the time-varying electromagnetic fields can be emitted from the surroundings of these high-power heating devices. Therefore, from the viewpoint of worker protection in a fusion facility, protection from non-ionizing radiation as well as ionizing radiation will be important. However, there is not enough research on non-ionizing radiation in fusion facilities, and it has not been taken up as an item in the fusion reactor safety research and reactor design [5, 6].

We have investigated a time-varying electromagnetic field around RF heating devices [7-9]. In the previous studies [8, 9], the monitoring equipment was placed at one point although the RF heating devices are installed over a wide area in the heating equipment room. Therefore, the behavior and distribution of electromagnetic fields around these devices were unknown. In this study, a new wide-area monitoring system, which enables multi-point simultaneous measurement, was developed and installed around the ICRF heating system of large helical device (LHD) as a test case to understand the behavior of the non-ionizing radiation around the megawatt-class amplifiers.

## II. ICRF System in LHD and Electromagnetic Field Monitoring System

### A. LHD and ICRF System

LHD at the National Institute for Fusion Science is the largest helical type fusion test device equipped with a superconducting magnet coil system. One of the major features of the LHD is the steady-state plasma operation. The LHD is equipped with vacuum pump systems, various heating devices and plasma diagnostic system. Since its initial operation in 1998, the LHD has been producing high-performance plasmas and the achievements in the LHD have led to the establishment of a helical system [10, 11]. The specification of LHD is summarized in Table1. In the LHD, the heating systems of several tens of megawatts have been installed as shown in Table. 1. Among these heating systems, the ICRF heating system has a maximum of 3 MW in one unit (two amplifier chains). Since the maximum magnetic field B is 3 T at the major radius, R = 3.9 m, the range of ion cyclotron resonance frequency for hydrogen plasma is tens of MHz, especially 30~40 MHz. The schematic diagram of the ICRF heating system for LHD is shown in Fig. 1. It consists of loop antennas, high voltage probes, stub tuners with a feedback control system for the real-time impedance matching for a long pulse, the coaxial transmission line, a directional coupler, the three-stage amplification system of wideband amplifier (WBA), driver power amplifier (DPA) and final power amplifier (FPA), RF-

TABLE I
Specifications of Large Helical Device [10, 11]

| Parameter | Nominal specification |
|---|---|
| Major radius of plasma, R | 3.9 m |
| Minor radius of helical coil | 0.975 m |
| Minor radius of plasma | 0.5 to 0.65 m |
| Magnetic field, B | 3 T at R = 3.9 m |
| Plasma volume | 30 $m^3$ |
| Magnetic energy | 0.9 GJ |
| Coil temperature | 4.4 K |
| Heating power | |
| ECRH | ~ 5.4 MW |
| ICRF | ~ 3 MW |
| NBI | ~ 28 MW |

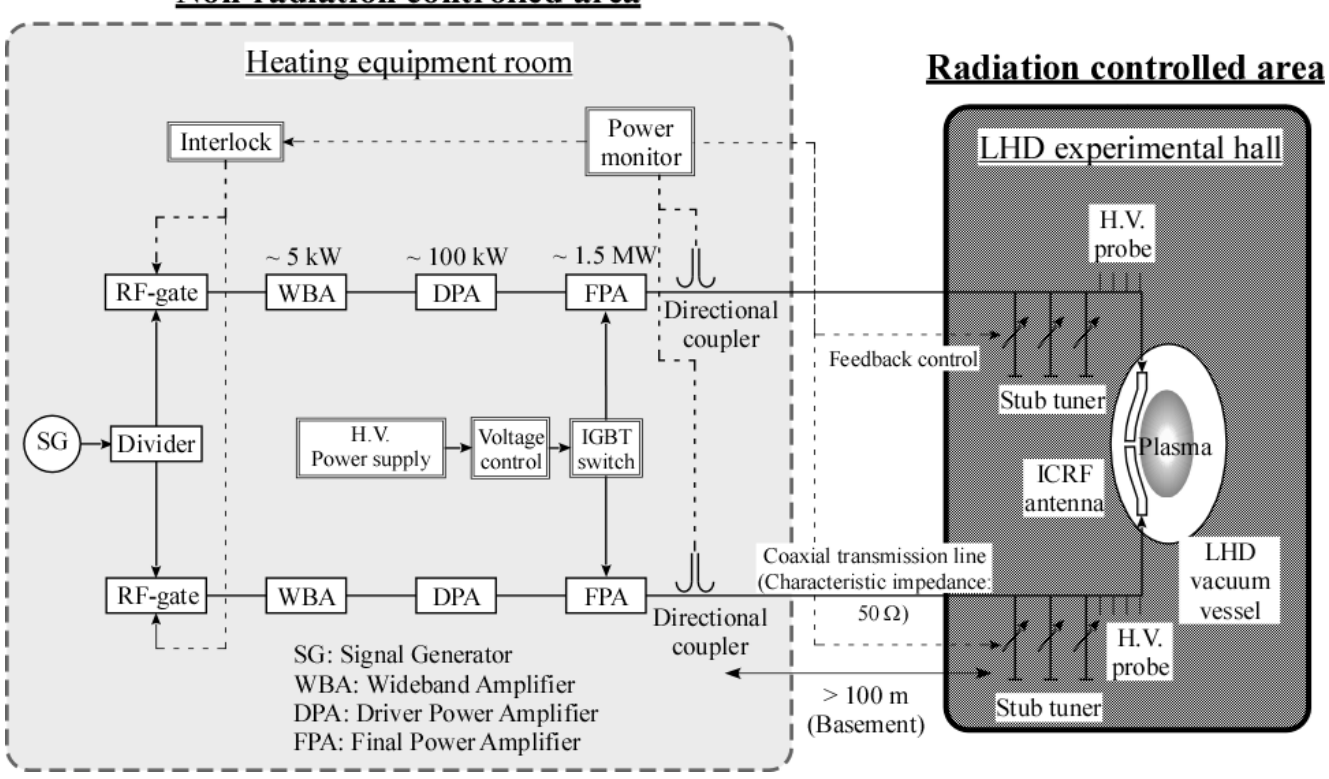


Fig. 1. Schematic diagram of ICRF heating system consisting of plasma, loop antennas, high voltage probes, stub tuners, coaxial transmission line, directional coupler, three-stage amplifier, RF-gate, signal generator, and interlock system [14].

TABLE II
SPECIFICATIONS OF MEASURING INSTRUMENT FOR AREA MONITORING

| Device | Nominal specification | |
|---|---|---|
| SRM-3000 (Narda S.T.S.) | Probe | 3581/01 |
| | Sensor type | Triaxial active magnetic loop |
| | Frequency range | 100 kHz to 250 MHz |
| | Dynamic range | 2.5 μA/m to 560 mA/m |
| | Averaging time | 0.96 s |
| | Operation modes | Spectrum analysis, time analysis |
| Radman (Narda S.T.S., Wandel Golterman) | Probe | ESM-20 (fast type) |
| | Sensor type | Magnetic and electric field Isotropic (triaxial) sensor |
| | Frequency range | H-field: 3 MHz to 1 GHz<br>E-field: 3 MHz to 7 GHz |
| | Averaging time | 0.03 s for electric field<br>1 s for magnetic field |
| | Dynamic range (30 MHz to 300 MHz) | 0 to 160 % (8.5 to 77.7 V/m) (Sensitivity: ~ 6 %*) (percent ratio to occupational Japan RCR STD-38) |
| | Probe | ESM-30 (slow type) |
| | Sensor type | Magnetic and electric field Isotropic (triaxial) sensor |
| | Frequency range | H-field: 3 MHz to 1 GHz<br>E-field: 3 MHz to 40 GHz |
| | Averaging time | 1 s |
| | Dynamic range (30 MHz to 300 MHz) | 0 to 160 % (0.03 to 0.206 A/m) (Sensitivity: ~ 6 %) (percent ratio to occupational Japan RCR STD-38) |

* The sensitivity of ESM-20 made by Wandel Golterman is less than 2 %.

gate system, a signal generator and an interlock system. The directional coupler and high voltage probes are installed in the transmission line. The loop antennas are installed in front of the plasma and are used for the injection of radiofrequency (RF) waves to plasma. High-power RF wave for ICRF heating is transmitted through long coaxial lines. These antennas are impedance matched efficiently using the stub tuners. Otherwise, the impedance matching between plasma and antennas may be inefficient and the reflected RF waves may return to the RF amplifier system. The RF amplifier devices can be a rather complex system which consists of a high-power tetrode, movable tuning stubs and a vacuum variable capacitor, etc. The detailed ICRF system is described elsewhere in [12-15].

### *B. Electromagnetic Field Monitoring System*

The loop antennas and stub tuners are installed in LHD radiation controlled area, while the ICRF power supply and amplification system are installed in the non-radiation controlled area. In the radiation controlled area, the worker's access is restricted during plasma experiments. Considering the safety of workers, therefore, we focused on measuring the leakage electromagnetic fields around an ICRF power supply system. This device was targeted because workers can approach the ICRF power amplifier system during the operation. In the previous study [8, 9], two EMC-300 (Narda Safety Test Solutions) with either electric or magnetic probes and SRM-3000 (Narda Safety Test Solutions) with the magnetic probe were installed at one point located a few meters from ICRF amplifiers. It could monitor the leakage electromagnetic field from ICRF devices. On the other hand, 8 FPAs have been extensively installed, and localized leakage electromagnetic field is a concern. Therefore, the construction of a multipoint electromagnetic field monitoring system is required from the viewpoint of workers' protection. The EMC-300 is often used for electromagnetic field measurement, but it is not suitable for multipoint monitoring because it is expensive. Hence, we have proposed using a handy personal RF monitor as an area monitoring instrument [16]. A personal RF monitor has many advantages, including cost-effectiveness, compact size, lightweight, isotropic response and standards compliance. Also, a personal RF monitor can simultaneously measure electric and magnetic fields. The specifications of the personal RF monitors are summarized in Table II along with SRM-3000. In this study, two types of personal RF monitors, Radman ESM-20 and ESM-30 (Narda Safety Test Solutions or Wandel Golterman), were used as electromagnetic field monitors. According to the Japanese occupational standard of the RCR STD-38, the dynamic range of Radman in the frequency range from 30 MHz to 300 MHz is 8.5 to 77.7 V/m and 0.03 to 0.206 A/m, respectively as shown in Table 2. The instrument is powered by a battery but was modified to use a DC power supply to enable continuous measurement for a long period.

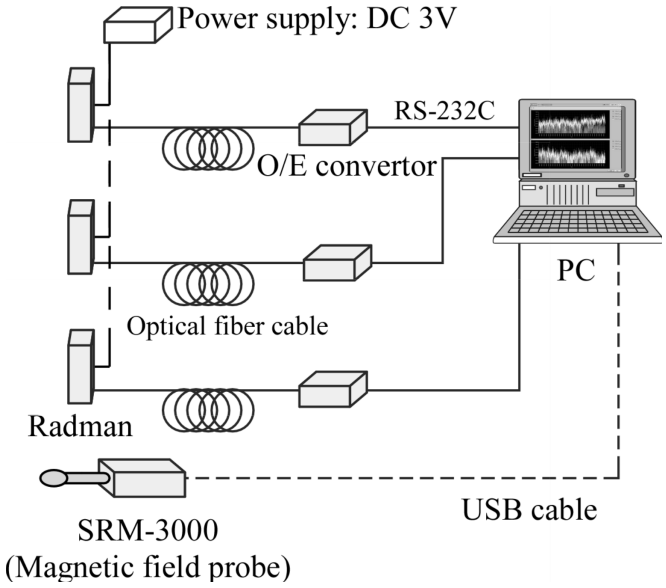


Fig. 2. The system configuration of data acquisition for the multipoint monitoring instruments.

The electromagnetic field strength standard should be applied as radiofrequency exposure protection guideline in the Japan RCR STD-38, when the distance between the source of the electromagnetic field and the worker exceeds 0.2 m. The reference levels for occupational exposure in the frequency range from 30 MHz to 300 MHz is 61.4 V/m and 0.163 A/m which are root mean square values averaged over 6 min. In the ICNIRP Guidelines [18], which are essentially consistent with the Japan RCR STD-38, the reference levels for occupational exposure in the same frequency range are 61 V/m and 0.16 A/m, whereas they are root mean square values averaged over 30 min. The measured value of Radman is the relative value in accordance with the reference levels in Japan RCR STD-38. Hence, the electric field strength, $IR_E$, is expressed by the

following equation:

$$IR_{\mathrm{E}}\,[\%] = \frac{E^2}{E_0^2} \times 100. \quad (1)$$

Here, $E$ is the measured electric field [V/m] and $E_0$ is the reference level of the Japan RCR STD-38. For the magnetic field, $IR_{\mathrm{H}}$ [%] is expressed as $H^2/H_0^2 \times 100$. All monitoring

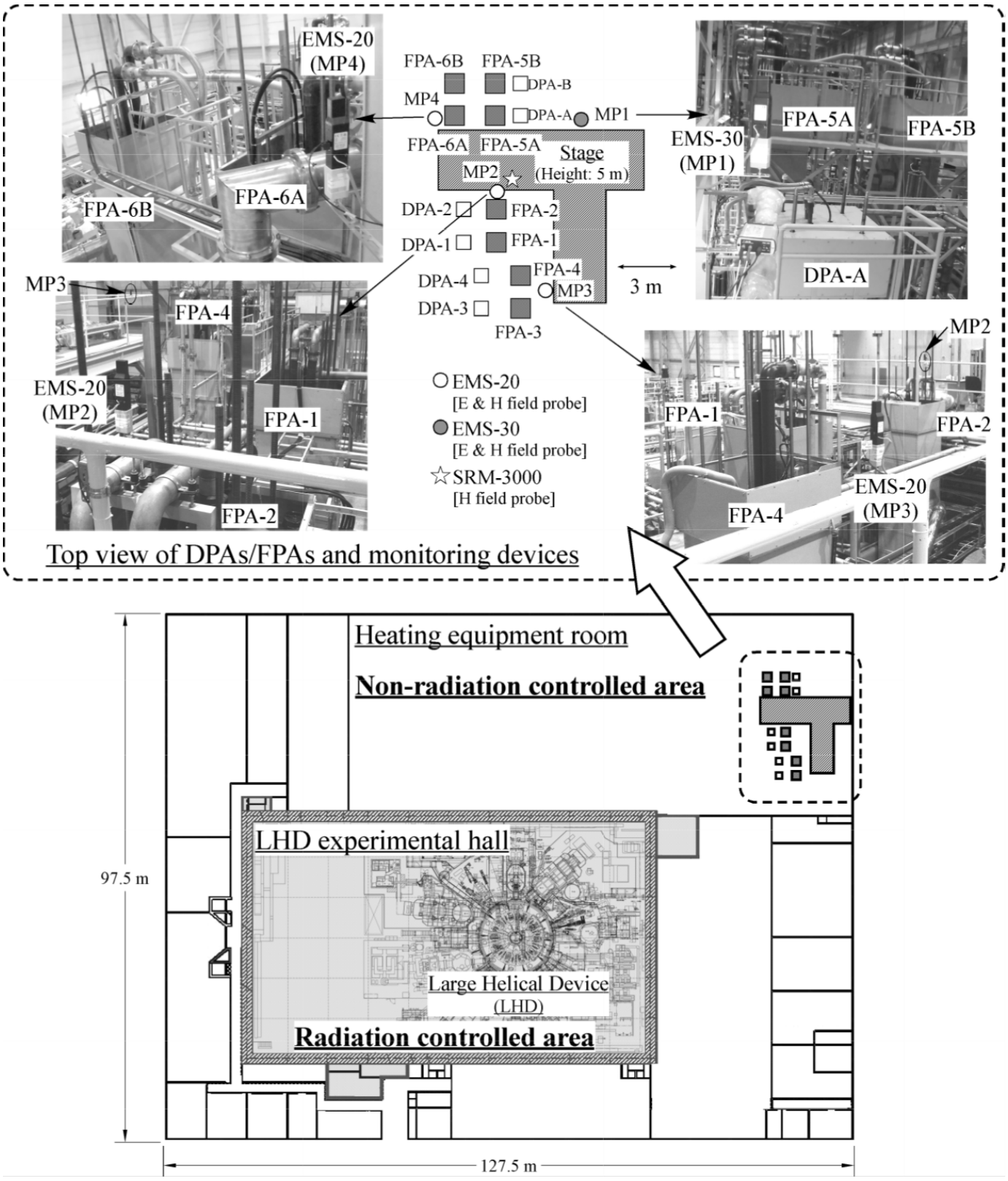


Fig. 3 Layout in the LHD experimental building and the monitoring devices around the ICRF amplifiers in the heating equipment room. The grey zoon in the LHD experimental building is the radiation controlled area. The other is non-radiation controlled area.

instruments were connected to a personal computer using fiber-optic or USB cables to acquire measurement data as shown in Fig. 2. An original multipoint measurement software was developed for monitoring. The time interval for data acquisition was 0.2 s, which is specified by the instrument.

The layout in the LHD experimental building and the monitoring devices around the ICRF amplifiers in the heating equipment room is shown in Fig. 3. In the results of preliminary observation, there is no large leakage electromagnetic field in the lower part of the FPA. Therefore, we set up a measuring device at a height of 5-6 m, which is almost the same as the top of the FPA and observed the electromagnetic field. The distance between the MP1 and the center of FPA-5A is about 5 m. The ESM-20 has been installed as an MP2 at a distance of about 0.6 m from the center of FPA-2 since 2011. The SRM-3000 was temporarily set up in the MP2 location. In the MP3, the ESM-20 has been installed at a distance of about 2.5 m from the center of each of FPA-4 and FPA-3 since 2011. In the MP4, the ESM-20 has been installed at a distance of about 1 m from the center for the FPA-6A since 2012. When the frequency of ICRF is 38.5 MHz, the wavelength $\lambda$ is 7.8 m and $\lambda/2\pi$ is 1.2 m. Thus, MP2 and MP4 are in the near-field region, MP1 and MP3 would be in the far-field region.

## III. Monitoring Results and Discussion

### A. Magnetic Field and Spectrum

The frequency, intensity and time variations of the electromagnetic field were observed with the SRM-3000. Here, we measured the leakage field from FPA-2 using a triaxial magnetic field probe. Fig. 4 shows the spectrum of the leakage magnetic field at a certain time. The frequency of ICRF waves was 38.47 MHz. The peak frequency of the observed leakage magnetic field was 38.47 MHz. The peak frequency was the same as the oscillation frequency of ICRF waves. Hence, the observed electromagnetic field would have leaked from the ICRF amplifiers. Fig.5 shows the time variation of leakage magnetic field from FPA-2 during ICRF operation in plasma experiment. The monitoring peak frequency of the SRM-3000 was fixed at 38.5 MHz. In these monitoring results, the leakage

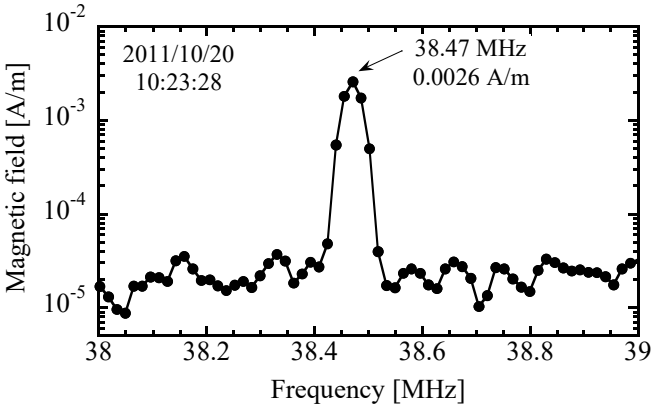


Fig. 4 A spectrum of the leakage magnetic field at a certain time by SRM-3000 with a magnetic probe.

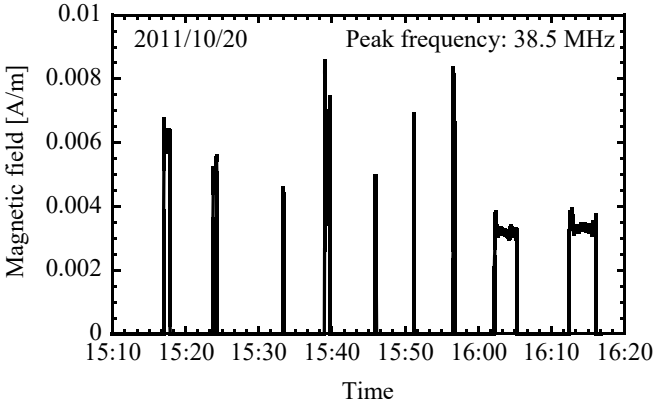


Fig. 5. The variation of leakage magnetic field from FPA-2 during ICRF operation in plasma experiment.

magnetic field intensity was less than 0.01 A/m. The leakage magnetic field around the ICRF amplifier is not large, because no magnetic field has been detected by the EMC-300 [8] or Radman so far.

### B. Electric Field

In this section, we discuss the correlation between the leakage electromagnetic field and the RF forward power $P_{fwd}$ and reflected power $P_{ref}$, focusing on the results measured with Radman. The RF forward power and reflected power were measured via the directional coupler installed at the output of FPA as shown in Fig. 1.

Fig. 6 shows the temporal variations of the leakage electric field at MP2, the RF forward power and reflected power by FPA-2, during 6 s discharge. The data of electric field by Radman are extracted from Fig. 6. The time interval for data acquisition of RF power and the voltage of the standing wave on the transmission line was 1 ms. Although the spike-like

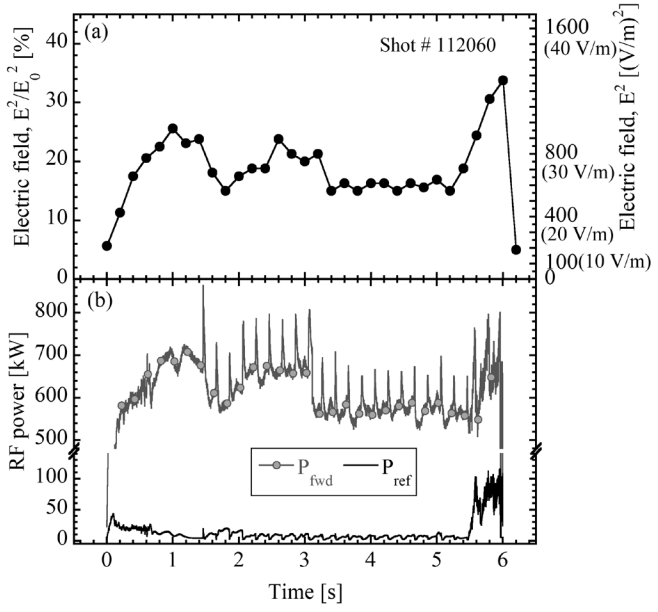


Fig. 6. The temporal variations of (a) the leakage electric field at MP2, (b) the RF forward power and reflected power.

fluctuations of few Hz are difficult to detect by Radman at MP2, the slow fluctuations of the leakage electric field can be sufficiently observed even at a time resolution of 0.2 s of Radman. The fluctuation of the leakage electric field is likely correlated with the RF forward power through FPA-2. Although the RF reflected power is much lower than the RF forward power, it may also influence the leakage electric field.

Fig.7 shows the results of ICRF operation and leakage electric field around the FPAs during long-pulse discharge operation more than 300 s. The time interval for data acquisition of RF power was 3 ms. The ICRF operation data were from FPA-2 and FPA-3. The leakage electric fields during the operation could be detected at the monitoring point of MP2 and MP3. The average leakage electric fields were approximately 17.6 % (25.8 V/m) and 2.0 % (8.7 V/m), respectively. At MP2, the behavior of the observed leakage electric field tended to be the same as the behavior of RF forward power. On the other hand, the leakage electric field at MP3 was lower than that the MP2. One of the reasons is that the MP2 is at a distance of several meters from the source of the electromagnetic radiation, the other is that the RF forward power of FPA-2 is an order magnitude higher than that of FPA-3. Nevertheless, Radman at MP3 catches the electric field coming from the FPA. The behavior of the leakage electric field at MP3 is similar to the variation of the RF reflected power of FPA-3. This implies that the Radman might detect the leakage electric field via the RF reflected power of FPA-3 even though the RF reflected power is much lower than the RF forward power.

### *C. Source of the leakage electromagnetic field in the ICRF heating system*

As for the cause of the leakage electric field, RF forward power was transmitted to the plasma by the coaxial transmission line, and RF reflected power was generated by the plasma load fluctuation, resulting in a leakage electric field. In the coaxial transmission lines of the ICRF system as shown in Fig. 1, the following locations are considered to be subject to leakage of the electromagnetic field: (1) connection point between ICRF antenna and transmission line, (2) installation location of electric field measurement probes in the transmission line, (3) movable coaxial liquid stub tuner, (4) connection point between the coaxial transmission line and directional coupler, (5) connection point between the coaxial transmission line and FPA, (6) the amplifiers of FPA, DPA and WBA. However, (1) to (3) are in a radiation controlled area and are more than 100 m apart from the monitoring area. Besides, in the measurement area of (4) to (6), the largest leakage electric field was observed near the FPA, so it can be inferred that the leakage source of the electromagnetic field would be the FPA, which has the largest RF power among these amplifiers.

Fig. 8 shows the schematic structure of the FPA referred from [12]. The Radman at MP2 is set near the top of FPA. The input impedance matching circuit for RF input from DPA (driver power amplifier) is located at the lower part of the FPA. The RF power is extracted via an external output coaxial transmission line. The directional coupler for the monitoring of RF forward and reflected powers is installed at the outlet of the FPA. The double coaxial output cavity is adopted for the FPA output cavity in the upper part of the FPA. The movable stubs (referred to as “Matching stub” and “Tuning stub”) are installed in the upper part of the FPA. The positions of movable stubs are adjusted using a dummy load before the operation and are fixed during the operation. The double coaxial cavity is made of a thin copper plate. The stub tuners are designed to move the shorting plate in the double coaxial cavity with the tuning rod. Metal contact fingers are adopted in the shorting plate. The wall current may leak out of the gap between the shorting plate and the double coaxial cavity wall and radiate the electric field through the tuning rod as an antenna.

The anode of the tetrode tube is attached to the inner

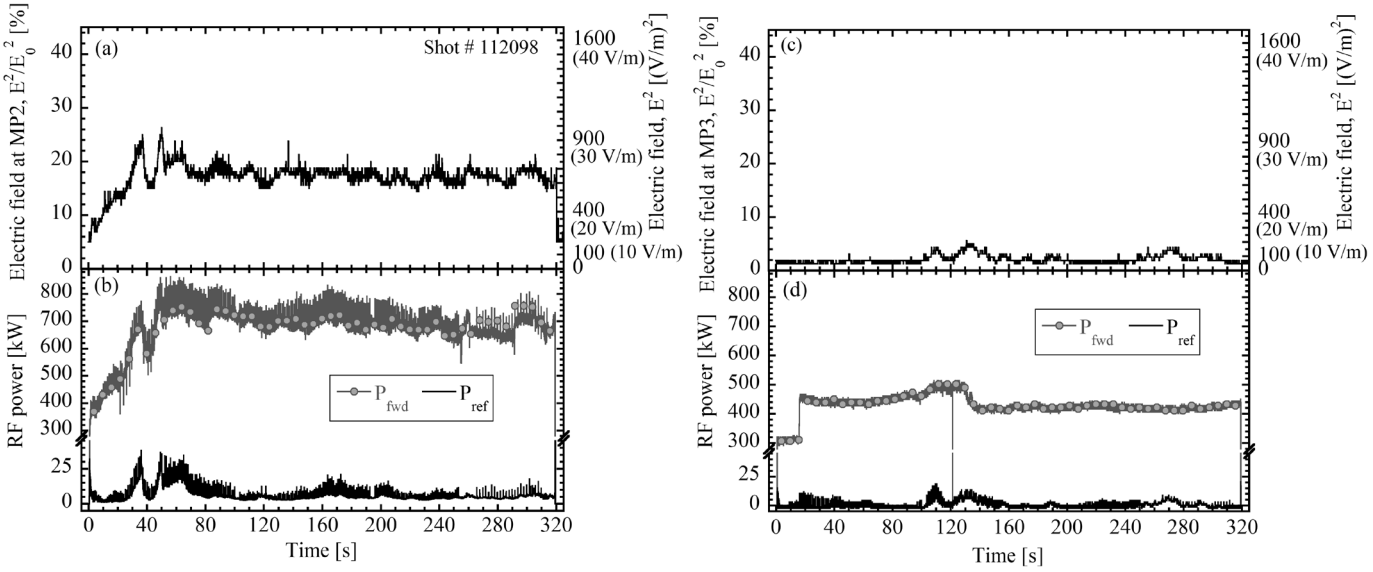


Fig. 7. The variations of the leakage electric field (upper), the RF forward power and reflected power (lower) for 320 s discharge. (a) and (b) are data from FPA-2 and the monitoring point of MP2. (c) and (d) are data from FPA-3 and the monitoring point of MP3 respectively.

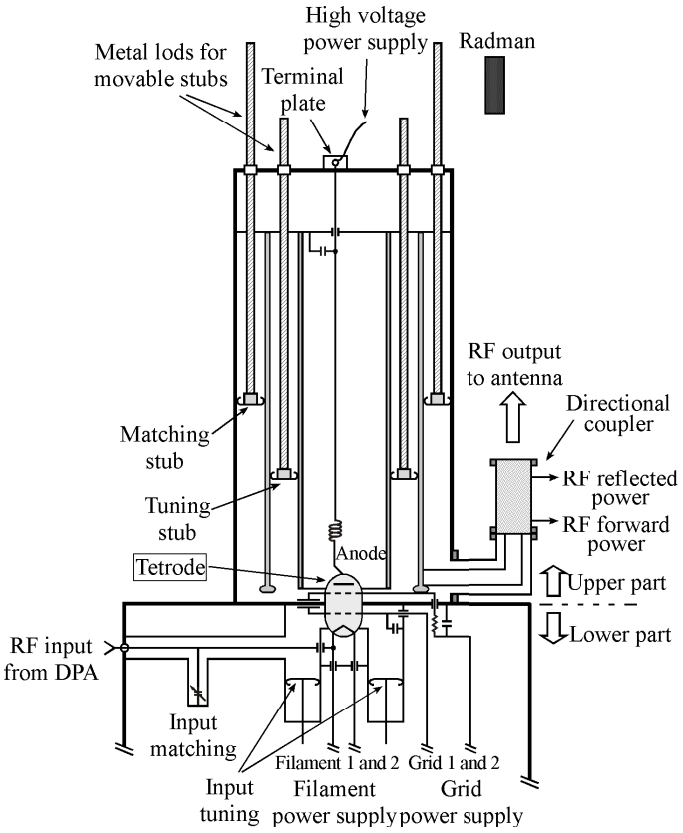


Fig. 8. Schematic structure of the FPA. A part of structure of FPA is revised and omitted from the figure in Ref. 12. The lower part is the input cavity, and the upper part is the output cavity. The directional coupler is installed at the RF output. The Radman at MP2 is set at the top level of FPA.

conductor through thin Teflon sheets. The high voltage power supply line to the anode is connected via the terminal plate at the top of the FPA. The RF power is transmitted from the anode (amplifier output) via the stub tuner in FPA and the directional coupler on a coaxial transmission line. Therefore, when a part of RF forward power is reflected by plasma load fluctuations, it returns to the anode of the tetrode and causes power fluctuations in the tetrode output, which may result in leakage of the electric field through the stub and/or the anode terminal of high voltage power supply at the top of the FPA. Detailed identification of the sources of the leakage electromagnetic field is a future issue.

### *D. Long-term monitoring results around the FPAs*

LHD plasma experimental campaigns were carried out mainly in the fall and winter. During the rest of the year, the LHD and heating devices were inspected for maintenance and then the devices were tested. Hence, year-round monitoring is important. Fig. 9 shows the daily maximum values of the leakage electric field measured from 2011 to 2015 at MP2, MP3 and MP4. The frequency of the ICRF is mainly 38.47 MHz throughout these experimental periods. The daily maximum values are not six minutes average value but the instantaneous values. The hatch indicates the plasma experimental period. In the plasma experiments, all the monitoring devices were able to detect the leakage electric field. It indicates that the proposed system is applicable to the monitoring of leakage electromagnetic fields in a wide area. The maximum leakage

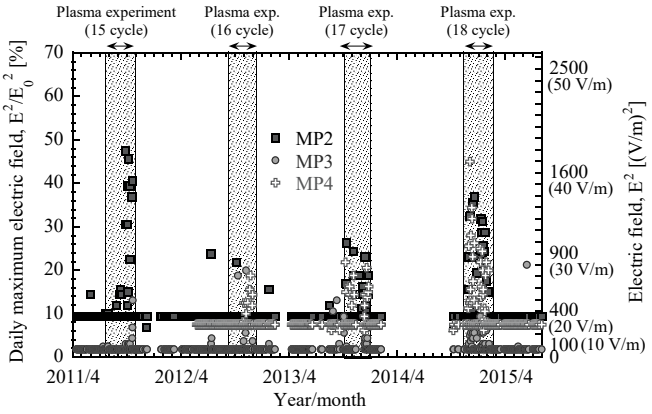


Fig. 9. The daily maximum values of the electric field measured from 2011 to 2015 at MP2, MP3, and MP4.

electric field of 42.3 V/m ($IR_E$ = 47.5%) was observed at MP2 during the plasma experiment on September 26, 2011. The reference level in the Japan RCR STD-38 is specified as a value that does not cause undesirable electromagnetic phenomena such as increase in core body temperature, electric shocks, radio frequency burns, etc. Thus, the observed electric field level around the FPAs is considered to have no influence on the human body.

### *E. Safety Issues for the Electromagnetic Field Management in Magnetic Confinement Nuclear Fusion Facilities*

According to the Japan RCR STD-38 and ICNIRP guidelines, the averaging time of 6 minutes and 30 minutes, respectively, is used to evaluate the electromagnetic environment. Current fusion test devices are operated in pulses of a few seconds or tens of seconds. Therefore, it is considered that there is no need to monitor the leakage electromagnetic field around the fusion test device. On the other hand, the LHD with superconducting magnetic coils can be operated for tens of minutes. Besides, the International Thermonuclear Experimental Reactor under construction in France will use 20 MW of ICRF power (frequency range: 40-55 MHz) in quasi-CW operation (pulses up to 3600 s) for a variety of plasma scenarios [19]. In the next generation of fusion devices, long-duration discharges using high-power RF waves will be performed. Therefore, it is important to establish safety management methods for non-ionizing radiation as well as monitoring of ionizing radiation from the viewpoint of ensuring the safety of workers. We believe that the multipoint wide area monitoring system proposed by us is applicable to larger fusion facilities.

## IV. Conclusion

The leakage electromagnetic field around the mega-watt class ICRF amplifiers in a magnetic confinement fusion test facility was observed by developed multipoint monitoring system using several electromagnetic field measurement instruments. It was found that the leakage magnetic field was less than the measurement sensitivity of the personal RF monitor. On the other hand, the leakage electric field could be clearly detected near the FPA. The leakage electric field in the

near-field region increases as the RF forward power increases and it would be radiated through the stub in the FPA and/or high voltage supply line connected to the anode of the tetrode. The maximum leakage electric field was 47.5% (42.3 V/m) of the reference value of the ICNIRP. The observed electric field level was considered to have no influence on the workers.

In the next generation of fusion devices, it is important to consider the electromagnetic compatibility and the protection of workers around the amplifiers, because the higher power amplifiers for ICRF system will be used for a long time. Thus, the proposed multipoint electromagnetic field monitoring system can be applied to wide area continuous measurements in a large fusion facility.

## ACKNOWLEDGMENT

The authors would like to thank Mr. S. Takami of the National Institute for Fusion Science for his technical support.

## REFERENCES

[1] T.J. Dolan, "Plasma heating and current drive," in *Magnetic Fusion Technology*, *Lecture Notes in Energy*, vol. 19, T.J. Dolan, Ed. London, UK: Springer-Verlag, 2013, pp. 175-232.

[2] M. Porkolab, *et al*., "Radiofrequency waves, heating and current drive in magnetically confined plasmas," in *Fusion Physics*, M. Kikuchi, K. Lackner and M.Q. Tran, Ed., Vienna, Austria, IAEA, 2012, pp. 609-755.

[3] A. Gibson and The JET Team, "Deuterium-tritium plasmas in JET, behavior and implications," *Phys Plasmas*, vol.5, pp. 1839-1847, 1998.

[4] J.D. Strachan, *et al*., "TFTR DT experiments," *Plasma Phys. Control. Fusion*, vol.39, pp. B103-114, 1997.

[5] T.J. Dolan and L.C. Cadwallader, "Safety and environment," in *Magnetic Fusion Technology*, *Lecture Notes in Energy*, vol. 19, T.J. Dolan, Ed. London, UK: Springer-Verlag, 2013, pp. 619-652.

[6] L.A. El-Guebaly and L.C. Cadwallader, "Recent developments in safety and environmental aspects of fusion experiments and power plants," in *Nuclear Reactor, Nuclear Fusion and Fusion Engineering*, A. Aasen and P. Olsson, Ed. New York, NY, USA: Nova Science Publishers, 2009, pp. 321-365.

[7] J. Wang, *et al*., "New approach to safety evaluation of human exposure to stochastically-varying electromagnetic fields," *IEEE Trans. Electromagn. Compat.*, vol. 47, pp. 971-976, Nov. 2005.

[8] M. Tanaka, *et al*., "A remote monitoring system of environmental electromagnetic field in magnetic confinement fusion test facilities," *IEEJ Trans. Fund. Mater*., vol. 130, pp. 451-456, May, 2010.

[9] T. Uda, *et al*, "Electromagnetic fields measurement and safety consideration in magnetic confinement fusion test facilities," *Plasma Fusion Res.,* vol. 7, Art. No. 2405085, 2012.

[10] A. Komori, *et al.*, "Goal and achievements of Large Helical Device project," *Fusion Sci. Technol*., vol. 58, pp. 1-11, July/Aug. 2010.

[11] Y. Takeiri, *et al*., "Extension of the operational regime of the LHD towards a deuterium experiment," *Nucl. Fusion*, vol. 57, no. 10, Art. No. 102023, 2017.

[12] T. Seki, *et al.*, "Steady state amplifier at megawatt level for LHD ICRF heating," *Fusion Sci. Technol*., vol. 40, pp. 253-264, Mar. 2001.

[13] S. Saito, *et al*., "Real-time impedance matching system for ICRF heating in LHD," *Fusion Eng. Des*., vol. 83, pp. 245-248, Apr. 2008.

[14] T. Mutoh, *et al.*, "ICRF heating system in LHD," *Fusion Sci. Technol*., vol. 58, pp. 504-514, July/Aug. 2010.

[15] T. Seki, *et al*., "Study of the antenna loading resistance of the LHD ICRF antenna," *Plasma Fusion Res*., vol. 5, Art. No. S2101, 2010.

[16] M. Tanaka, *et al.*, "Performance test of personal RF monitor for area monitoring at magnetic confinement fusion facility," *Radiat. Prot. Dosimetry*, vol. 148, no. 3, pp. 277-283, 2012.

[17] Radio Frequency-Exposure Protection Standard, RCR STD-38, Japan, the Association of Radio Industries and Businesses, 1999.

[18] "ICNIRP guidelines for limiting exposure to electromagnetic fields (100 kHz to 300 GHz)," *Health Phys*., vol. 118, no. 5, pp. 483-524, Mar. 2020.

[19] P. Lamalle, *et al*., "Status of the ITER ion cyclotron heating and current drive system," *AIP Conf. Proc.*, vol. 1689, 2015, Art. No. 030007, DOI. 10.1063/1.49367

**Masahiro Tanaka** received the B.E. degree in applied physics from Osaka City University, Osaka, Japan in 1995, the M.E. degree in energy engineering and science and the D.E. degree in nuclear engineering from Nagoya University, Nagoya, Japan, in 1997 and 2005, respectively.

From 1997 to 2006, he was a semiconductor engineer at MITSUBISHI ELECTRIC Corporation, and a laboratory assistant at Nippon Kucho Service Co., Ltd. He joined the National Institute for Fusion Science (NIFS) in 2006 as a Research Associate. Since 2012, he has been an Associate Professor with the division of device engineering and applied physics, department of helical research, NIFS. From 2014, he was an Associate Professor with the department of fusion science, the Graduate University for Advanced Studies, SOKENDAI. His research interests include the tritium science and technology for nuclear fusion, environmental radioactivity, applications of microwave technology, safety management of ionization and non-ionization radiation.

Dr. Tanaka was a recipient of the Atomic Energy Society of Japan, Fusion Engineering Division, Young Scientist Award in 2008, and the International Symposium on Electromagnetic Compatibility Excellent Paper Award in 2009.

**Tetsuo Seki** received the B.S., M.S., and Ph.D. degrees in physics from Nagoya University, Nagoya, Japan in 1988, 1990, and 1993, respectively.

Since 1993, he has been a Scientific Staff with the National Institute for Fusion Science, Gifu, Japan and working on the heating system and experiment of ion cyclotron range of frequency heating in fusion plasma research.

**Jianqing Wang** (M'97, SM'19, F'21) received the B.E. degree in electronic engineering from the Beijing Institute of Technology, Beijing, China, in 1984, and the M.E. and D.E. degrees in electrical and communication engineering from Tohoku University, Sendai, Japan, in 1988 and 1991, respectively.

He was a Research Associate with Tohoku University, and a Senior Engineer with Sophia Systems Company, Ltd. In 1997, he joined the Nagoya Institute of Technology, Nagoya, Japan, where he has been a Professor since 2005. He has authored Body Area Communications (Wiley-IEEE) in 2012.

Prof. Wang received the IEEE EMCS Technical Achievement Award in 2019. His current research interests include biomedical communications and electromagnetic compatibility.

**Yoshitsugu Kamimura** (S'83-M'85) received the B.E., M.E. and Ph.D. degrees in electrical engineering from Nagoya University, Nagoya, Japan, in 1980, 1982 and 1985, respectively.

From 1985 to 1991, he was a scientist at Communications Research Laboratory, Tokyo, Japan, where he carried out research in electromagnetic compatibility. Since 2011, he is a Professor of Department of Information Science at Utsunomiya University, where he has worked in biological effects of electromagnetic fields and electromagnetic compatibility.

Prof. Kamimura received the Shinohara Memorial Young Investigators Award from IEICE in 1989, and the Best Paper Award from JAMIT (Japanese Society of Medical Imaging Technology) in 1999.

**Tatsuhiko Uda** received the Bachelor degree of pharmaceutical sciences and Master degree of agricultural sciences from Kyoto University, Kyoto, Japan in 1970 and 1972, respectively, and the Doctorial degree of engineering from Tokyo Institute of Technology, Tokyo, Japan in 1987. From 1972 to 1994 working about development of nuclear engineering at Hitachi Ltd. and Japan Atomic Energy Research Institute (JAERI). From 1994 to 2012 he worked at National Institute for Fusion Sciences (NIFS) as professor, where his major topics are study and management of radiation safety including nonionizing radiation.

In 2012 he retired the NIFS and given the Professor emeritus of NIFS and the Graduate University for Advanced Studies, SOKENDAI.

His recent interesting is safety consideration for ionizing and nonionizing radiation in atomic energy and radiation facilities.

**Osamu Fujiwara** (M'83-L'17) received his B.E. degree in electronic engineering from Nagoya Institute of Technology, Nagoya, Japan, in 1971, and his M.E. and D.E. degrees from Nagoya University, Nagoya, Japan, in 1973 and 1980, respectively, both in electrical engineering.

From 1980 to 1984, he was with the Department of Electrical Engineering, Nagoya University as a Research Associate, and from 1984 to 1985 as an Assistant Professor. In 1985, he joined the Nagoya Institute of Technology as an Associate Professor. In 1993 he became a Professor with the Graduate School of Engineering. In 2012 he retired and was awarded Emeritus Professor from National University Corporation, Nagoya Institute of Technology. His research interests include bioelectromagnetics and electromagnetic compatibility. He served as Chair of IEICE EMCJ from 2009–2010, IEEJ TEMC from 2002–2004, IEEE EMC Chapter of Japan Council from 2004–2005 and IEEE Nagoya Section from 2005–2006, a member of International Advisory Board for Physics in Medicine and Biology from 2009-2012, an Associate Editor of the IEEE EMC Transactions from 1992-2012, and an Associate Editor of the IEEE EMC Newsletter from 1998-2012.

Dr Fujiwara is a Fellow of the IEEJ, a life fellow of the IEICE, and an IEEE life member. He received IEEE EMC Society Honored Member Award in 2016, and is the recipient of Distinguished Paper Awards in 1980 and 2000 from the IEEJ and the IEICE, respectively, Technical Development Award in 2013 and Achievement Award in 2014 all from the IEEJ.